

# X-Ray Optics and Diagnostics for the First Experiments on the Linac Coherent Light Source

*A. Wootton, J. Arthur, T. Barbee, R. Bionta, R. London, H.-  
S. Park, D. Ryutov, E. Spiller, R. Tatchyn*

This article was submitted to  
46<sup>th</sup> Annual Meeting and Exhibition and Education Program, San  
Diego, CA, July 30-August 2, 2001

*U.S. Department of Energy*

Lawrence  
Livermore  
National  
Laboratory

**June 13, 2001**

## DISCLAIMER

This document was prepared as an account of work sponsored by an agency of the United States Government. Neither the United States Government nor the University of California nor any of their employees, makes any warranty, express or implied, or assumes any legal liability or responsibility for the accuracy, completeness, or usefulness of any information, apparatus, product, or process disclosed, or represents that its use would not infringe privately owned rights. Reference herein to any specific commercial product, process, or service by trade name, trademark, manufacturer, or otherwise, does not necessarily constitute or imply its endorsement, recommendation, or favoring by the United States Government or the University of California. The views and opinions of authors expressed herein do not necessarily state or reflect those of the United States Government or the University of California, and shall not be used for advertising or product endorsement purposes.

This is a preprint of a paper intended for publication in a journal or proceedings. Since changes may be made before publication, this preprint is made available with the understanding that it will not be cited or reproduced without the permission of the author.

This work was performed under the auspices of the United States Department of Energy by the University of California, Lawrence Livermore National Laboratory under contract No. W-7405-Eng-48.

This report has been reproduced directly from the best available copy.

Available electronically at <http://www.doc.gov/bridge>

Available for a processing fee to U.S. Department of Energy  
And its contractors in paper from  
U.S. Department of Energy  
Office of Scientific and Technical Information  
P.O. Box 62  
Oak Ridge, TN 37831-0062  
Telephone: (865) 576-8401  
Facsimile: (865) 576-5728  
E-mail: [reports@adonis.osti.gov](mailto:reports@adonis.osti.gov)

Available for the sale to the public from  
U.S. Department of Commerce  
National Technical Information Service  
5285 Port Royal Road  
Springfield, VA 22161  
Telephone: (800) 553-6847  
Facsimile: (703) 605-6900  
E-mail: [orders@ntis.fedworld.gov](mailto:orders@ntis.fedworld.gov)  
Online ordering: <http://www.ntis.gov/ordering.htm>

OR

Lawrence Livermore National Laboratory  
Technical Information Department's Digital Library  
<http://www.llnl.gov/tid/Library.html>

# X-ray optics and diagnostics for the first experiments on the Linac Coherent Light Source

A. Wootton<sup>\*</sup>, J. Arthur<sup>b</sup>, T. Barbee, R. Bionta, R. London, H-S. Park, D. Ryutov, E. Spiller and  
R. Tatchyn<sup>b</sup>

Lawrence Livermore National Laboratory, P.O. Box 808, Livermore, CA 94550, USA;

<sup>b</sup>Stanford Synchrotron Radiation Laboratory, Stanford Linear Accelerator Center, Stanford, CA 94305,  
USA

## ABSTRACT

The Linac Coherent Light Source (LCLS) is a 1.5 to 15 Å-wavelength free-electron laser (FEL), currently proposed for the Stanford Linear Accelerator Center (SLAC). The photon output consists of high brightness, transversely coherent pulses with duration < 300 fs, together with a broad spontaneous spectrum with total power comparable to the coherent output. The output fluence, and pulse duration, pose special challenges for optical component and diagnostic designs. We discuss some of the proposed solutions, and give specific examples related to the planned initial experiments.

Keywords: free electron laser, x-ray optics, x-ray diagnostics

## 1. INTRODUCTION

The DOE Office of Basic Energy Science (OBES) has endorsed research and development (R&D) towards a fourth-generation light source<sup>1</sup> based on a LINAC-driven x-ray free electron laser (XFEL)<sup>2</sup>. Critical Decision 0, a statement of mission need, was signed on 13 June 2001. Such an XFEL would operate in an entirely new physics regime, Self-Amplified Spontaneous Emission (SASE), which has been now made possible by demonstrated advances in producing low-emittance electron beams (for a list of SASE-related experimental results, see <http://www-ssrl.slac.stanford.edu/lcls/>). The OBES is now funding R&D to develop a specific proposal, the LINAC Coherent Light Source (LCLS)<sup>3,4</sup>, which would utilize the last third of the SLAC LINAC and a precision undulator to produce keV x-rays with unprecedented brilliance. By adding a high intensity short pulse laser to the proposed LCLS experimental hall, pump/probe techniques promise insight into the dynamic structural response of many forms of matter on time scales from 10 fs to ms and on spatial length scales from Angstroms to microns. Atomic physics, warm dense matter physics, femto-second chemistry, nano-scale dynamics in condensed matter, and biological applications have been highlighted for the first experiments<sup>5</sup>. Many others are possible.

The unprecedented brightness of the source highlights demanding requirements as well as innovative design opportunities for optical systems, diagnostics and components to transport the beam to the experiment stations. A comprehensive design review is available<sup>6</sup>. Figure 1 illustrates the problem<sup>1</sup>; normal energy fluences ( $\text{J. cm}^{-2}$ ) at the undulator exit far exceed those

---

Contact: [\\*wootton1@llnl.gov](mailto:*wootton1@llnl.gov); phone (925) 422 6533

<sup>1</sup> optical quantities are taken from the CXRO home page at <http://www-cxro.lbl.gov/>, and physical constants from the CRC Handbook of Chemistry and Physics, 65<sup>th</sup> edition.

require to melt most materials. The problem is somewhat alleviated downstream, where the natural divergence of the beam ( $1 \mu\text{rad}$  at 8 keV,  $10 \mu\text{rad}$  at 1 keV) reduces the fluence.

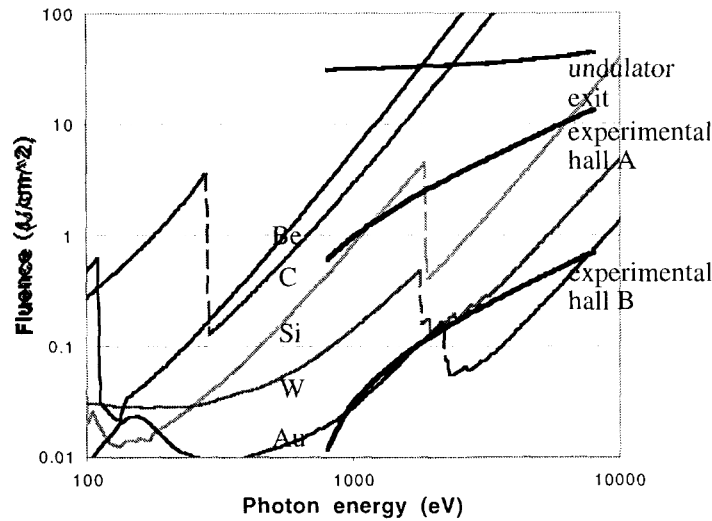


Figure 1. Normal incidence fluences from the LCLS coherent radiation beam, together with fluences required to bring various materials to their melting temperature (Be, C, Si, W, and Au). The phase change energy is not included. Curves are shown for the LCLS coherent beam at the undulator exit, and at positions representative of the two experimental halls.

A working assumption for precluding material damage that would affect x-ray properties is:

*‘There will be no changes to material x-ray properties during the x-ray pulse, and no irreversible changes at any time, as long as the fluence is kept < about 1/2 that required to bring the material temperature to melt’.*

This assumes that long-time (i.e. > photon pulse length) irreversible processes such as phase changes (e.g. graphitization of C in multilayers, melt), spallation, and plastic deformation are precluded by keeping the material temperature below half the melting temperature, and that there are no short time (< photon pulse length) reversible or irreversible changes during the pulse itself. These assumptions are being explored, both theoretically and experimentally.

Specific hardware solutions that reduce the normal fluences shown in Figure 1 to values consistent with the working assumption above are:

- a) a far field experimental hall to reduce energy densities by natural divergence,
- b) a gas absorption cell to continuously attenuate by  $> 10^4$ ,
- c) low-Z optics that are damaged least (e.g. a phase zone plate for warm dense matter experiments),
- d) grazing incidence optics that increase the optical footprint and reflect most incident power.

Part of the strategy of the LCLS x-ray optics working group is to utilize an example of each of the above four solutions early in the experimental program, to gain experience. Should these hardware solutions be insufficient, two other solutions are being explored. First, multi-phase optics whose surfaces can be continuously replenished have been considered. Initial liquid and plasma lens studies are complete. Second, there is always the solution of dynamic solid state optics, that are spatially translated between shots.

## 2. A FAR FIELD HALL

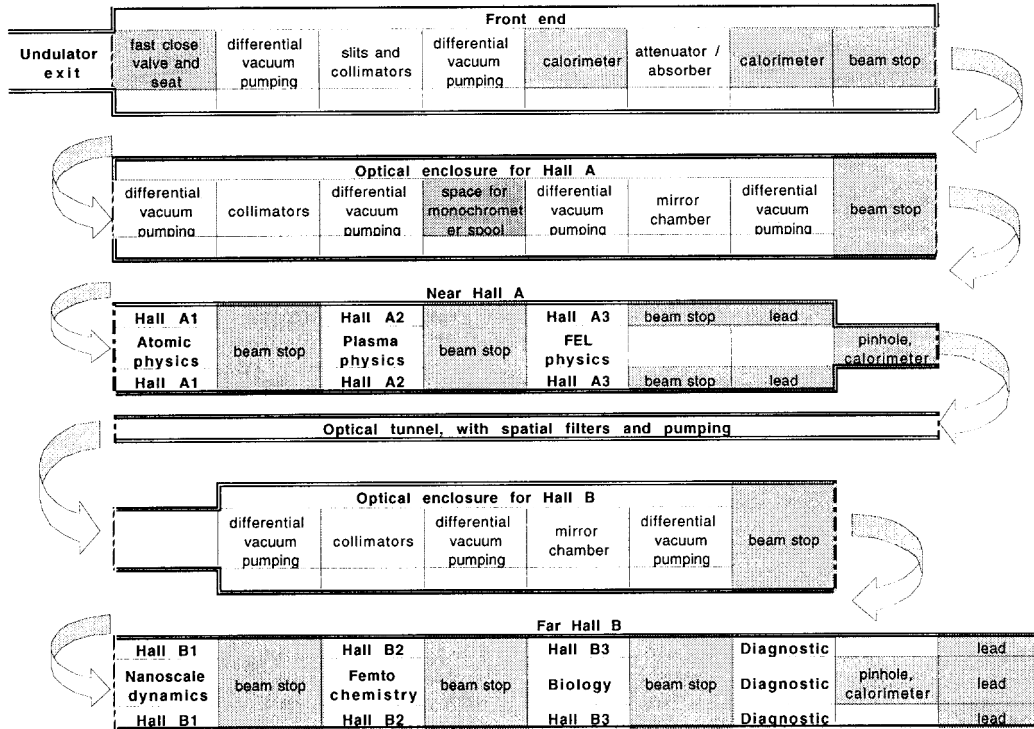


Figure 2. An illustration of one experimental layout being considered. The two main experimental halls, A and B, are separated by an optical tunnel. Optical halls are used for providing attenuation and energy filtering. The initial experiments planned are indicated.

One experimental layout under consideration is illustrated by Figure 2, showing the location of an absorption cell, take-off mirrors or crystals, horizontally and vertically tunable x-ray slits, pumping sections, collimators, etc. Two main experimental halls are provided, one close to the undulator exit (Hall A, starting ~ 50 m from the undulator end) and one downstream of the undulator (Hall B, starting ~ 400 m from the undulator end). Optics in Hall B experience a reduced fluence, by about a factor 15 (see Figure 1), allowing many standard solutions and materials to be applied. Hall A is necessary because a number of the optical elements and instruments developed depend on close proximity to the LCLS undulator for optimal operation or parameter values. These include:

- planar take-off mirrors (if these were 300 m farther downstream they would need to be substantially longer, up to 1 meter/facet);
- refractive lenses (whether solid state or gaseous, such lenses are efficiency-limited by their aperture diameter; even at distances of ~50 m from the undulator their operation will be marginal);
- chirped-multilayer compressor optics (these are efficiency-limited by the beam diameter);
- multilayer-based transmission gratings (with present techniques it is doubtful that the required high-quality and efficient gratings with apertures greater than ~100  $\mu\text{m}$  could be built).

An additional reason for a close hall (Hall A) involves the transmission of the spontaneous synchrotron radiation (SR) to experiments. Close to the undulator, a ~1 cm aperture through the vacuum system should transmit a usable fraction of this spectrum. This aperture is at the limit at which the differential pumping systems we have specified can operate effectively. In order to transmit the same SR cone to the far hall, the vacuum aperture would more than double, necessitating a significantly more expensive vacuum system.

The large flight distance to Hall B, and associated beam wander, is not expected to be a problem. The angular acceptance for SASE saturation through the undulator is of the same order as the beam divergence, so any beam angle excursions larger than this value would probably quench any coherent output (a similar constraint applies to the position of the beam axis). Active monitor and feedback system coupled to positional and attitude controls on the mirrors (and possibly the undulator) are planned to help stabilize beam movement.

### 3. A GAS ABSORPTION CELL

Attenuation of the beam is accomplished by passage through a gaseous, solid, or liquid medium. While all have been considered, the nominal design, shown in Figure 3, is for a gas cell<sup>7</sup> operated with high pressure puff valves to introduce the absorbing gas into the path of the coherent FEL photons. At the lower photon energies, gas must be used as all solid materials will melt. One possibility under consideration is to use a mixed attenuation scheme; gas for initial attenuation, followed by low Z (e.g. Be) for further attenuation. This would have the advantage of reducing the gas handling requirements.

The axial dimensions and the number of valve nozzles must allow a sufficient depth of the gas to provide four or more orders of magnitude of attenuation over the full range of the LCLS fundamental (~0.8 to 8 keV). The combined axial and transverse dimensions are determined by the requirement of maintaining an average vessel pressure of <0.0075 Torr, corresponding to the Knudsen-through-molecular flow regimes<sup>8</sup>. This pressure, (for N<sub>2</sub>) is sufficiently low to be reduced to <10<sup>-6</sup> Torr by the differential pumping sections bracketing the chamber.

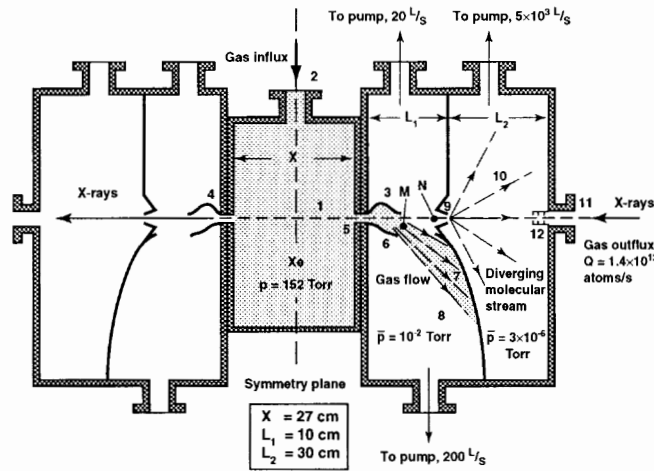


Figure 3. The conceptual design for the gas cell absorber.

### 4. LOW-Z OPTICS

From Figure 1, we see that low-z transmissive optics may be used at the higher photon energies even at the undulator exit; even with 100% absorption and normal incidence the lowest Z materials will not melt. Phase zone plates, produced by sputtering and then slicing, have already been successfully used<sup>9</sup> in the hard x-ray regime (> 5 keV), so that their use is considered a variant on a proven technique.

Low-Z transmissive optics are well suited for the focusing element for the low temperature plasma/warm dense matter (WDM) experiments<sup>3</sup>. Here the LCLS XFEL beam will be used to heat and ionize thin solid samples to produce solid density plasmas, whose properties will then be measured by an array of diagnostics placed around the sample. Latter

experiments will use a laser to produce the plasma, and the FEL beam as a probe. The first plasma experiment requires the highest energy photons at 8.275 keV, to penetrate as deeply as possible into the sample. The heated volume, approximately a cylinder, requires a radius of  $>5 \mu\text{m}$  in order to create a large enough sample for study. The fluence required to bring the sample to the energy required (electron temperature  $T_e \sim 10 \text{ eV}$ ), over the volume  $V$  defined by the thickness (equal to the penetration depth of the photons) and the minimum  $5 \mu\text{m}$  radius, is calculated from a simple energy balance. No energy escapes the sample on the time of the FEL pulse, so the plasma energy equals the FEL pulse energy. The Saha equation is solved by iteration to calculate the ion density  $n_i$  and the ionization state  $I_p^i$  of stage  $i-1$ ,:

$$\frac{E}{V} = \frac{3}{2}kn_eT_e + \sum_i n_i I_p^i$$

It is sufficient to assume single ionization,  $2/3$  of the FEL pulse energy deposited,  $n_i = n_e$ , and  $I_p^i = 6 \text{ eV}$ . The result is that the FEL beam must be focused to a spot diameter  $\sim 10 \mu\text{m}$ , with a lens efficiency  $> 0.5$ , to achieve the required plasma states in Al. The use of focusing optics adds additional requirements for alignment, which include the ability to image the spot at the position of the sample and the capability of running at high repetition rates at reduced intensity during the alignment process.

The chosen focusing optic is a variant of a blazed Fresnel zone-plate (a Fresnel lens) operating like a thin lens in visible optics. The lens forms an image of the XFEL source at the sample. The source-to-lens and lens-to-image distances determine its focal length. The XFEL source point is at the position of the waist in the Gaussian model which is located one Rayleigh length upstream of the exit of the undulator. The source-to-lens distance is 92.8 m, and the lens-to-image distance is 5 m, requiring a lens focal length of 4.74 m and giving a magnification of 0.05.

Figure 4 shows details of the design. The lens is carved into the face of a C disk and mounted over a hole drilled through a 25.4 mm diameter Cu mount. The C disk is  $650 \mu\text{m}$  thick except in the center, where it thins down to  $400 \mu\text{m}$ . The active portion of the lens is  $200 \mu\text{m}$  in diameter and consists of 6 concentric grooves machined to a maximum depth of  $18.8 \mu\text{m}$ . The plot of the beam profile at the lens, Figure 4g, shows that the  $200 \mu\text{m}$  lens diameter captures most of the beam.

The shape of the grooves was determined by calculating the phase change necessary to convert the diverging Gaussian XFEL beam from the undulator to a converging Gaussian waveform whose waist is at the sample position. The radial phase profile was converted to a depth profile by multiplying by the optical constant for C which, at 8.275 keV, is  $18.8 \mu\text{m} / 2\pi$ .

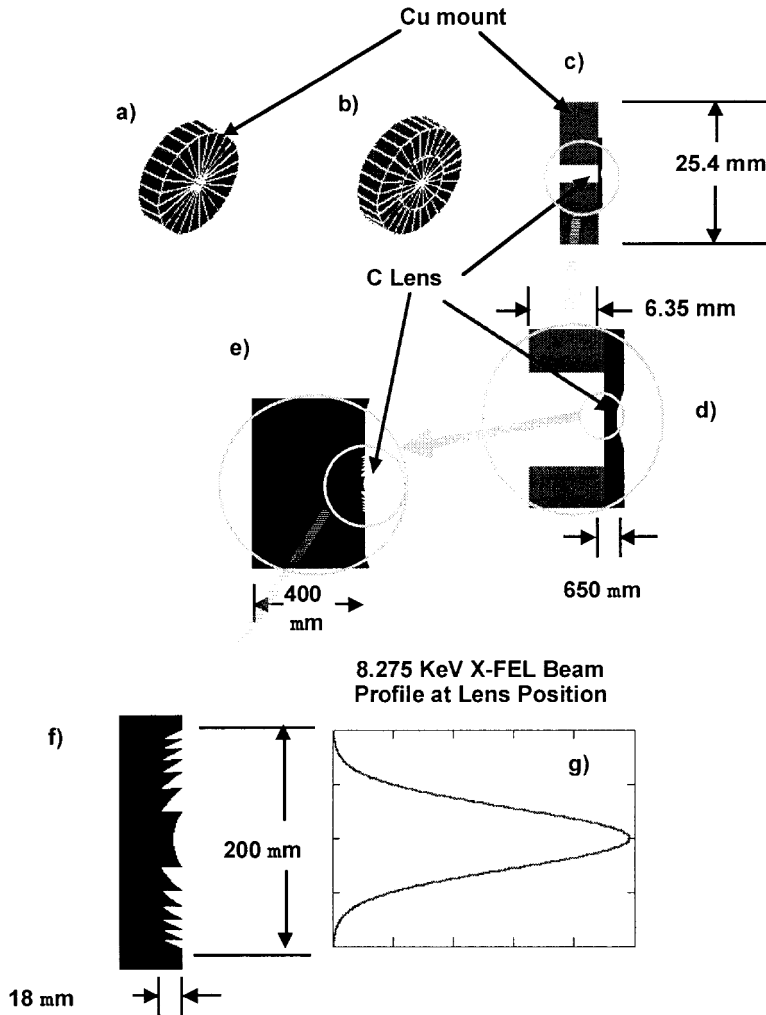


Figure 4. Details of the warm dense matter (plasma experiment) lens design. a) the Cu mount, b) the Cu mount and lens, c) another view of the mount and lens, d) an enlarged view of the center part of the mount and lens, e) the C lens (before thinning), f) detail of the lens surface, g) the FEL beam profile shown on the same vertical scale as the lens detail in f.

## 5. GRAZING INCIDENCE OPTICS

The atomic physics experiments<sup>5</sup> will use the LCLS photons at  $\sim 1$  keV (for highest inner shell cross sections, and to satisfy energy thresholds) to create multiple core hole states, to investigate non-resonant two-photon ionization of the L shell, and to study giant Coulomb explosions. The first experiments will be on core hole formation, requiring that two photons be absorbed by the K shell before Auger relaxation occurs. A beam focused to a spot diameter  $0.1 \mu\text{m}$  has been requested, although a larger diameter ( $1 \mu\text{m}$ ) may be acceptable. Apertures may be used to remove spontaneous radiation, and a grazing incidence mirror used as a filter to remove higher harmonics (e.g. the third harmonic at 2.4 keV when the fundamental is 0.8 keV). Here we consider the focusing system.

Figure 1 illustrates that, at the location of Hall A, focusing with a transmissive lens might be possible using the lowest Z materials. However the margin of safety is very small, and with multiple shots the temperature increase becomes a problem.

Instead we propose to use grazing incidence mirror geometry; an ellipsoidal or paraboloid surface focusing in two dimensions. The absorbed energy per atom is given by<sup>6</sup>

$$\eta = \frac{E_{beam} \sin(\theta_i)(1-R)}{d_w^2 \delta n_a}$$

Here  $E_{beam}$  is the beam energy per pulse,  $d_w$  the beam diameter at the optic,  $\theta_i$  the grazing incidence angle,  $\delta$  the penetration depth (approximated by the maximum of the 1/e penetration depths of the light and subsequent photo-electrons) into the material in a direction normal to the surface,  $n_a$  the atomic density of the material, and  $R$  the reflection coefficient. As the grazing angle is decreased the reflectivity term  $(1-R)$  and the footprint term  $\sin(\theta_i) / d_w^2$  decrease the absorbed energy density. Until the critical angle is reached (from above) the penetration depth decreases, so this term increases the absorbed energy density.

The material is chosen to accommodate the high fluence, so must be low Z. Figure 5 shows the ratio of energy absorbed per atom at a given grazing angle to that absorbed for normal incidence, for Si at both 0.8 and 8 keV. Large reductions are possible below the grazing angle. Including an estimate for the photo-electron penetration depth shows that an order of magnitude reduction from the marginally safe energy load is possible at 1 degree.

The proposed design is for a Be, C or Si paraboloid lens with grazing incidence angle 1 degree, distance to focus of 1 m, and thus a radius  $r = \sqrt{1.2188 \times 10^{-3} z}$  (m) (= 3.5 cm at the center of the beam). The full-width-half-maximum beam diameter, ~ 650  $\mu\text{m}$  for 1 keV photons at the experimental location, implies a mirror length ~ 7 cm. To achieve the 0.1  $\mu\text{m}$  spot diameter implies a surface finish ~ 5 nm, a maximum slope error ~  $0.5 \times 10^{-7}$  rad, and a maximum tilt of the axis of  $1 \times 10^{-5}$  rad. The maximum slope error, beyond state of the art, is relaxed present capabilities for the 1  $\mu\text{m}$  spot diameter.

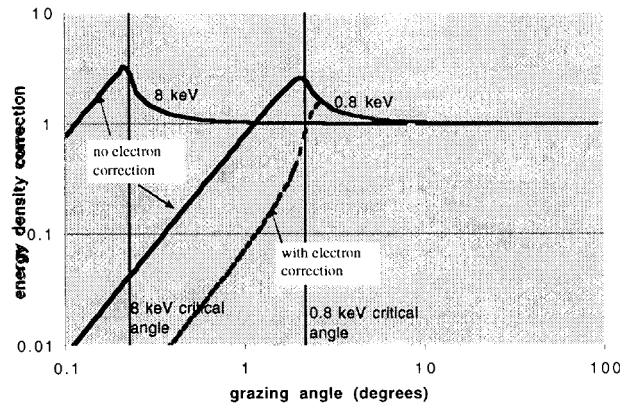


Figure 5. The multiplicative factor on the tolerable fluence as a function of grazing incidence angle, for a plane Si surface irradiated by 800 and 8000 eV photons. For 800 eV the results are shown with and without a correction for photo-electron penetration. The critical angles are marked as vertical lines.

Two techniques are considered for manufacturing the optic. First only that part of the paraboloid that will reflect the photons can be constructed, i.e. a section ~ 7 cm long by ~ 1 mm wide. This can be made by numerical machining, an expensive process if large numbers of lenses are required. Alternatively full paraboloids can be made by sputter depositing layers of materials (e.g. Be, or C) onto a super-smooth mandrel, thus forming an optic from the inside outward. When the mandrel is separated from the sputtered foil, the innermost layer replicates the mandrel smoothness and serves as the reflecting surface.

The focusing element is thus a tube that is open at both ends, as shown in Figure 6. X-rays enter one end, undergo a single reflection at the interior surface, and exit from the other end with a different direction of travel. It may also be possible to form a Si optic using a mandrel rotated into a Si block. If required a beam block is can be used to stop any direct non-reflected x-rays from exiting the optic.

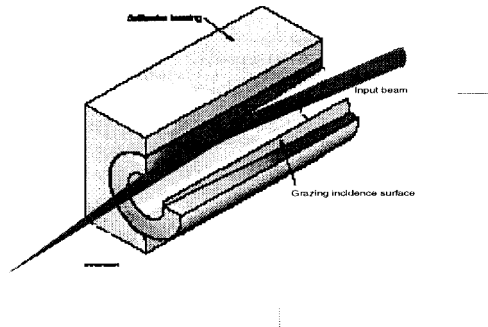


Figure 6. A schematic drawing of a replicated paraboloid lens, used for focusing.

Stress-relieved specular (and if required multilayer) reflecting surfaces and supporting electroplated shells do not deform during the separation process and consequently produce super-smooth surfaces comparable to the initial mandrel surface (i.e.  $rms \approx 3$  to  $4.5 \text{ \AA}$ ) with figures replicating the mandrel figure. In principle, single layer specularly reflecting surfaces only require that the total thickness of the single reflecting media layer be controlled for effective reflection performance to be achieved. In practice, it is necessary to maintain surface roughness and composition at levels which are technically required for effective performance. Calibration, in this case, requires only a quantitative knowledge of the layer thickness deposited on the replication mandrel surface under specified deposition source and replication mandrel motion conditions. Typical specular reflecting material structures are between 25 nm and 50 nm thick.

## 6. DIAGNOSTICS

Based on the list of initial experiments, a set of common usage diagnostics has been developed. They are categorized as either needed for measuring the coherent radiation properties, or the spontaneous radiation properties. For each they include:

- Spectrum (Low energy: grating spectrometers. High energy: crystal spectrometers)
- Energy (Accurate, intrusive: calorimetry. Monitor every pulse: ionization chamber)
- Profile, divergence, pointing, (Accurate and monitor: x-ray CCD camera)

As an example, a scheme being considered for the x-ray CCD camera to measure profile, divergence and pointing is shown in Figure 6a. A small fraction of the x-ray FEL beam is reflected by a thin foil of a low Z material such as Be, acting as a beam splitter, onto a doped YAG crystal<sup>10</sup>. Fast framing CCD cameras, suitable for recording the data, exist today.

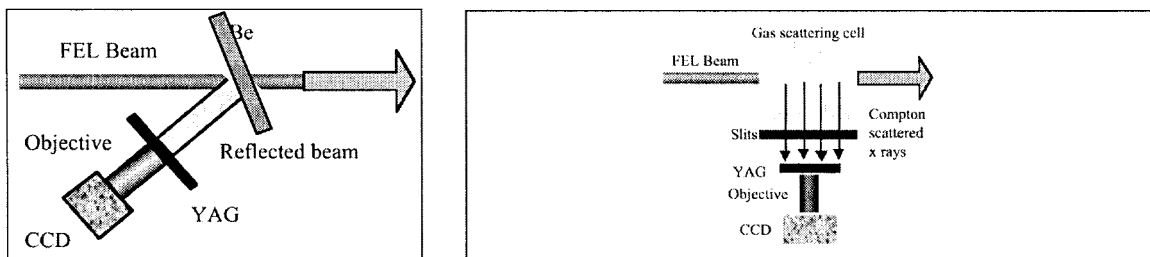


Figure 6. a) A schematic picture of a foil used as part of a detection system for characterizing beam profile and pointing. b) A schematic of a proposed technique to measure beam width using Compton scattering from a gas cell.

X rays are reflected from both front and rear surfaces of the foil. A suitable grazing angle is determined by the interplay between reflectivity, and reflection sensitivity to surface roughness. The foil thickness is determined by absorption, loss of spatial resolution caused by the shift of the images produced by reflections from the front and the rear sides of the foil, and incoherently, isotropically scattered light. The relative importance of this scattered light is reduced by increasing the distance between foil and detector. Fluorescence of heavier impurities can be mitigated in a similar manner. The most important issue is the foil quality. For example, if the surfaces of the film are wavy, then the images created by reflection from the two surfaces are distorted. Typically the two sides of the foil must be parallel to better than 40  $\mu$ rad. This planarity constraint must be satisfied on the scale  $\sim$ 2 mm, corresponding to the large axis of the beam imprint on the reflecting foil.

An alternate scheme, illustrated in Figure 6b, utilizes Compton scattering from a supersonic jet. Imaging is via a pinhole or slit, and again the detector is a YAG crystal and CCD camera. A thick Be foil may also be used as the scattering element.

Challenges remaining to be overcome include the measurement of temporal distribution, the measurement of coherence (an asymmetric Michelson interferometer has been suggested for this measurement<sup>6</sup>), and the measurement of the relative timing between the FEL beam and a laser when they are used in pump-probe configurations.

## SUMMARY AND CONCLUSIONS

The Linac Coherent Light Source is a proposal for the first in a new class of light sources. The unprecedented brightness implies a high energy loading on optics and diagnostics, and offers the opportunity for design innovations. Optics designs, have been presented involving the use of a far-field experimental hall, a gas absorption cell, low-Z optics, and grazing incidence optics. Part of the R&D strategy is to utilize an example of each type of optical design early in the experimental program, to gain experience. Should these be insufficient, optics whose surfaces can be continuously replenished have been considered (e.g. liquids and plasmas). There is also the solution of dynamic solid state optics, that are spatially translated between shots. Concerning diagnostics, we have given an example of the research and development being pursued for one, namely that required to measure beam pointing, profile and energy. There are many challenges remaining, for example how to measure pulse duration, and synchronization.

## ACKNOWLEDGEMENTS

This work was performed under the auspices of the U.S. Department of Energy by the University of California, Lawrence Livermore National Laboratory under Contract No. W-7405-Eng-48.

## REFERENCES

1. Report of the Basic Energy Sciences Advisory Committee, Panel on Novel Coherent Light Sources, January 1999, available at: [http://www.er.doe.gov/production/bes/BESAC/NCLS\\_rep.PDF](http://www.er.doe.gov/production/bes/BESAC/NCLS_rep.PDF).
2. J. B. Murphy and C. Pellegrini, "Introduction to the Physics of the Free Electron Laser," in *Frontiers of Particle Beams*, M. Month, S. Turner, eds., Lecture Notes in Physics No. 296, H. Araki et al, eds., Springer-Verlag, Berlin, pp. 163-212 (1988).
3. M. Cornacchia et al., "Performance and design concepts of a free-electron laser operating in the x-ray region," *SPIE Proceedings* **2988**, p2, (1997).
4. J. Arthur et al., *LCLS Design Study Report*, Internal Stanford University report SLAC-R-521, Rev. December 1998 UC-414 (1998).
5. *LCLS, The First Experiments*, available at: [http://www-ssrl.slac.stanford.edu/lcls/papers/LCLS\\_experiments\\_2.pdf](http://www-ssrl.slac.stanford.edu/lcls/papers/LCLS_experiments_2.pdf).

6. R. Tatchyn , J. Arthur, R. Boyce, T. Cremer, A. Fasso, J. Montgomery, V. Vylet, D. Walz, R. Yotam , A. K. Freund, M. R. Howells "X-ray Optics Design Studies for the 1.5-15 Å Linac Coherent Light Source (LCLS) at the Stanford Linear Accelerator Center (SLAC)", Paper Presented at the 1997 SPIE Annual Meeting, August 1, 1997, San Diego, CA; ms. #3154-22; *SPIE Proc.* **3154**; pp. 174-222 (1998).
7. D. Ryutov and A. Toor, "X-ray Attenuation cell". LCLS technical note 00-10, and LLNL internal report UCRL-ID-138125 (2000).
8. S. Dushman, *Scientific Foundations of Vacuum Technique*, John Wiley, New York, 1941.
9. R. Bionta, K. Skulina and J. Weinberg, "Hard x-ray sputtered-sliced phase zone plates", *Applied Phys. Letts.* **64** pp. 945-947 (1994).
10. A. Koch, C. Raven, P. Spanne, A. Snigrev, "X-ray imaging with sub-micrometer resolution employing transparent luminescent screens", *J. Opt. Soc. Am.* **15** pp. 1940-1951 (1998).